Topical Mydriatics Affect Light-Evoked Retinal Responses in Anesthetized Mice

Deb Kumar Mojumder and Theodore G. Wensel

Purpose. To characterize effects of the muscarinic antagonist atropine (A) and the α-adrenergic agonist, phenylephrine (P), on mydriasis and light-evoked signaling in mice anesthetized by ketamine and xylazine (K+X).

Methods. Pupillary areas of anesthetized C57BL/6 mice were measured, with or without topical application of A or A+P. Dark-adapted ERGs were recorded from 2- to 4-month-old C57BL/6 and 7.5-month-old albino *hrhoG/hrhoG* mice after application of A or P singly or in combination, before or after induction of K+X anesthesia. Effects of GABA were tested in the *hrhoG/hrhoG* mice.

Results. K+X anesthesia resulted in maximum mydriasis that was not enhanced by A or A+P. Dark-adapted b-wave amplitudes (−1.3 log sc td s) after K+X anesthesia were similar with or without A or P. A+P in the presence of K+X produced a slow growth in b-wave amplitude, reaching a plateau of twofold enhancement in 1 hour. Recordings of responses to varying flash energies revealed that the effects of A+P were on the maximum amplitude of the a- and b-waves and not on their sensitivity. Scotopic threshold responses were augmented as well. In photoreceptor-degenerated mice (*hrhoG/hrhoG*), an electronegative ERG wave recorded with K+X+A, was converted to a γ-aminobutyric acid (GABA)-sensitive response with two electropositive components with A+P after K+X.

Conclusions. Topical administration of A and P together, but not separately, in the presence of K+X, leads to a slow, dramatic enhancement of a- and b-waves by an unknown mechanism independent of pupil dilation. (*Invest Ophthalmol Vis Sci.* 2010;51:567–576) DOI:10.1167/iovs.09-4168

Mydriatics, pharmacologic agents used to dilate the pupils of the eye, are a requirement for many diagnostic and therapeutic procedures in ophthalmology (for review, see Ref. 1). Selective α-adrenergic agonists such as phenylephrine (a synthetic analogue of epinephrine) produce contraction of the radial muscles of the iris, causing pupillary dilation. Muscarinic receptor antagonists such as atropine or tropicamide, on the other hand, relax the circular muscles to dilate the pupils (for review, see Ref. 2). These agents can diffuse throughout the anterior structures of the eye and into the systemic circulation, so that even at the low doses used for topical instillation, mydriatics can enter the systemic circulation to affect remote organs, such as the heart and lungs.[3,4]

Anesthetics are necessary for various diagnostic, therapeutic, and surgical interventions in humans and animals. Of the different anesthetics used, a combination of ketamine, an NMDA (*N*-methyl-D-aspartate) receptor antagonist,[5] and xylazine,[6] an α2-receptor agonist, are used in a variety of species. Electroretinograms (ERGs) are routinely recorded in mice by using combinations of atropine and phenylephrine for mydriasis, and, ketamine and xylazine for anesthesia (for review, see Refs. 7, 8 The mouse has become one of the most widely used models for studying mammalian vision, largely because of the ease with which the mouse genome can be manipulated. The use of genetically altered mice has led to an increased understanding of molecular mechanisms of visual function in the retina. These models have provided insight into the mechanisms of retinal dysfunction degeneration and have and allowed development of new therapeutic interventions. Interpreting in vivo mouse retinal physiology in normal or pathologic states requires the recording and interpretation of their electroretinograms, which require the development of a consistent protocol for their recording to make interpretation dependable and comparable across laboratories.

A previous study reported that there was no significant difference in pupillary mydriasis in anesthetized mice tested with several commonly used topical mydriatics.[9] In contrast, another study mentioned the need for a combination of topical α-adrenergic agonist (2.5% phenylephrine HCl) and a muscarinic receptor antagonist (tropicamide 5 mg/mL) for maximal pupillary dilation and optimal electroretinogram amplitudes in anesthetized mice.[8] In optimizing procedures for our studies of ERG in knockout mice,[10] we noted that a combination of the muscarinic antagonist, atropine, and phenylephrine was needed to obtain maximum b-wave amplitudes, but their application did not seem to affect the light sensitivity of the responses, as would be expected for an effect primarily due to mydriasis. Therefore, we undertook an investigation of the effects of these drugs on pupil dilation and ERG responses in mice.

Methods

Animals

Pupillary measurements and electroretinograms were recorded in 25 adult C57/BL6 mice between 2 and 4 months of age. In addition, electroretinograms were recorded in 7.5-month-old albino mice (C57BL/6-Tyr$^{c\text{-}Brd}$ background) whose native rhodopsin gene had been replaced with the corresponding human DNA modified to encode an enhanced GFP fusion at the C terminus of rhodopsin (*hrhoG/hrhoG* mice[11]). All mice were reared and housed in a room with a 12-hour light (<40 lux)–12-hour dark cycle. All animal procedures conformed to U.S. Public Health Service and Institute for Laboratory Animal Research guidelines and were approved by the Baylor College of Medicine Institutional Animal Care and Use Committee. The experimental

From the Verna and Marrs McLean Department of Biochemistry and Molecular Biology, Baylor College of Medicine, Houston, Texas.

Supported by NIH Grant R01-EY11900 (TGW) and Welch Foundation Grant Q0035.

Submitted for publication June 17, 2009; revised July 24, 2009; accepted July 26, 2009.

Disclosure: **D.K. Mojumder**, None; **T.G. Wensel**, None

Corresponding author: Theodore G. Wensel, Department of Biochemistry and Molecular Biology, One Baylor Plaza, Baylor College of Medicine, Houston, TX 77030; twensel@bcm.tmc.edu.

procedures were in accord with principles of the ARVO Statement for the Use of Animals in Ophthalmic and Vision Research.

Recording Pupillary Diameter

Mice, previously dark-adapted overnight, were anesthetized with a loading dose of ketamine (77 mg/kg) and xylazine (16 mg/kg) (both drugs from Vedco, Inc., St. Joseph, MO) administered intraperitoneally and maintained with ketamine (56 mg/kg), and xylazine (12 mg/kg) administered SC. A first maintenance dose was administered after 40 to 45 minutes, and additional doses were administered if needed. The animal's head was positioned on a well-illuminated elevated platform and optimally positioned to be photographed with a mounted camera (SLR EOS Digital Rebel Digital camera; Canon USA., Inc., Lake Success, NY) fitted with an 60-mm f/2.8 (EF-S; Canon USA., Inc.) macro lens focused at the plane of the pupillary aperture. A transparent cylinder made of polypropylene with ultrathin side walls (outer diameter, 8 mm; height, 5 mm) was placed on the skin surrounding the eye and centered on the cornea. The cylinder was filled with 90 μL 0.25% sodium carboxymethyl-cellulose solution (Advanced Vision Research, Woburn, MA), to ensure that the cornea was kept well hydrated, the anterior-chamber was maintained throughout the photography session, and the limbus was clearly visible (Fig. 1A). The transparency of the cylinder ensured proper illumination of the pupillary plane. Topical mydriatics (20 μL each of 1% atropine sulfate; Bausch and Lomb Inc., Tampa, FL) and 2.5% phenylephrine HCl (Akorn, Inc., Buffalo Grove, IL) were instilled into this liquid bath. The filament bulbs that were used to provide illumination for photography provided sufficient heat to the animal, and no extra heating pads were used. The average rectal temperature at the end of the recording session was ~37.5°C to 38°C. Image capture by the camera was computer controlled at a 0.008-Hz frequency (Utilities RemoteCapture software, ver. 2.7.5; Canon USA., Inc.).

ERG Recording

A custom-built instrument and a procedure described previously[10] were used. Animals were dark-adapted overnight in a ventilated light-tight box. The next day they were prepared for recording under red illumination (LED, $\lambda > 620$ nm). The mice were initially anesthetized with an intraperitoneal injection of ketamine (77 mg/kg) and xylazine (14 mg/kg; both drugs from Vedco, Inc.). The first dose of maintenance anesthesia, ketamine (56 mg/kg) and xylazine (11.2 mg/kg) was administered after ~45 minutes, via a subcutaneous needle fixed to the flank, and subsequent doses were given when required. Slow administration of maintenance anesthesia (0.1 mL in 1 minute) did not

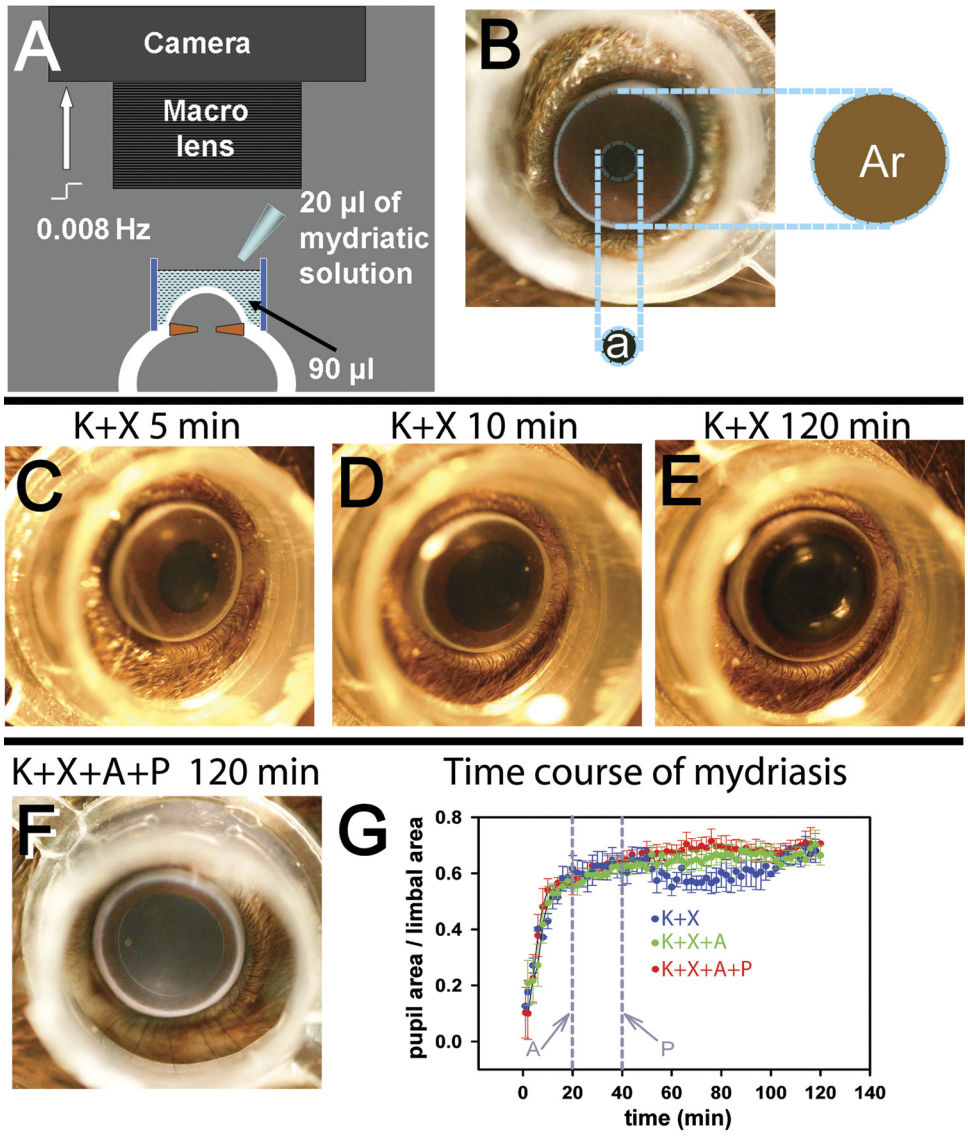

FIGURE 1. Measurement of pupillary mydriasis. **(A)** The setup used for recording pupillary mydriasis. A digital-SLR camera fitted with a macro lens was focused at the pupillary plane of the anesthetized mouse eye. A transparent polypropylene cylinder (outer diameter, 8 mm; height, 5 mm) was centered on the cornea and filled with 90 μL 0.25% sodium carboxymethyl-cellulose solution, to which 20 μL of mydriatic solution was added. The camera was computer controlled to take images at 0.008 Hz. **(B)** Photograph of a mouse eye showing that pupillary area (a) was expressed as a ratio of the area encircled by the limbus (Ar). **(C–E)** Representative photographs of a single mouse eye, showing levels of mydriasis 5, 10, and 120 minutes after K+X anesthesia. **(F)** Representative photograph of a mouse eye, taken 120 minutes after K+X anesthesia and topical A+P administration (topical A, 20 minutes, and topical P, 40 minutes after induction of anesthesia). **(G)** Time course of average mydriasis expressed as a ratio of the limbal area, produced by K+X anesthesia ($n = 4$), K+X anesthesia followed by A administered at 20 minutes from induction of anesthesia ($n = 3$) and K+X anesthesia followed consecutive administration of A at 20 minutes and P at 40 minutes from induction of anesthesia ($n = 4$). *Vertical gray lines*: time at which A and P were administered.

produce any significant alteration in the ERG waveform during continuous recording.

Rectal temperature was maintained between 36°C and 37°C with an electrically heated blanket (CWE, Inc., Ardmore, PA). The animal was housed in an aluminum Faraday cage, to insulate the recorded signals from external static electrical fields. An aluminum head holder with a hole for the upper incisors to fix the upper jaw held the animal's head steady, to reduce noise originating from respiratory and other movements. This fixation ensured that the jaw remained open throughout the recording. Moist room air was pumped through a clear PVC pipe kept close to the open mouth. The head holder also served as the ground. All animals were allowed to recover after the ERG recording session.

Recording of ERGs was started at ~20 minutes after administration of the loading dose and the sessions lasted up to 4 hours. The ERGs were recorded differentially between DTL fiber electrodes[12] moistened with normal saline and placed on the two eyes. The eyes were covered with contact lenses that were pressure molded from 0.19 mm clear film (ACLAR; Ted Pella, Inc., Redding, CA) for the stimulated eye and 0.7-mm opaque PVC for the nonstimulated eye (for details, see Ref. 13). Both lenses were placed over a cover of 1.2% methylcellulose in 1.2% saline. The signals were amplified (DC to 500 Hz), digitized at 2 kHz, and sent to the computer for averaging, display and storage, and subsequent analysis.

A custom-made LED (λ_{max}, 462 nm; −5.8 to 1.9 log sc td s)-based stimulator provided the light stimuli.[10] The maximum stimulus pulse width was <5 ms for all normal pigmented C57/BL6 mice but was incremented to 10 ms for the *hrhoG/hrhoG* mice, to get recordable signals. The light was collected in a cone internally coated with white paint and sent through a fiber-optic cable (0.5 in. diameter, 36 in. long; Edmund Optics, Barrington, NJ) into the Faraday cage. A diffuser and a stainless-steel cone at the distal end of the fiber-optic cable, kept very close to the stimulated eye, provided a Ganzfeld stimulus. ERGs were recorded with brief full-field flashes in darkness. The half-time of the pulse width was taken as time 0 for the ERG recording. Flash energy was varied by doubling the pulse width of the stimuli and by choosing banks of preattenuated LEDs.

Topical mydriatics were administered to both eyes under dim red illumination (LED, $\lambda > 620$ nm) with minimal displacement of the contact-lens and the DTL fiber electrode by apposing a drop of the mydriatic solution to the side of the contact lens. The solution was drawn into the tear film between the contact lens and cornea by capillary action, and the excess fluid was removed by absorbing it with a cotton-tipped applicator. ERGs were recorded after waiting ~5 minutes after instillation.

Intravitreal Injection

Injections were performed with a trinocular stereo articulating, flexible-boom-arm dissecting microscope (6.6× magnification) under dim red illumination (> 620 nm) to avoid light-adapting the rods. Pharmacologic agents were delivered via a 26-gauge stainless steel needle with a conical style noncoring point fixed on a 10-μL microsyringe (Hamilton Co., Reno, NV) and inserted at a 45° angle, into a small pilot hole 0.5 mm behind the limbus (created by a 30-gauge needle). To suppress inner retinal signaling, GABA (1–1.5 μL; final concentration of 35 mM based on an estimated vitreal volume of 20 μL) dissolved in balanced salt solution buffered close to pH 7.4 was delivered slowly over 1 minute to avoid excessive local concentrations. This concentration of GABA was found previously to suppress inner retinal ERG responses (Saszik S et al. *IOVS* 2002;43:ARVO E-Abstract 1817). After injection, the ERG was monitored until the waveform was stable (~40–45 minutes) before the recording was accepted.

Tissue Preparation

Retinal tissues were prepared in a manner similar to that detailed in previous publications.[14,15] Briefly, light-adapted adult *hrhoG/hrhoG* mice were used for immunohistochemical analysis. After ERG recording, the animals were euthanized by carbon-dioxide inhalation and the eyes were rapidly excised from the head. The corneas were slit open, the lens was expressed, and the eyes were immersed in 4% formaldehyde in 0.1 M cacodylate buffer (pH 7.4) for 5 minutes at 4°C, during which time gentle traction was used to peel the retina from the sclera. The vitreous humor was removed, and relaxing cuts were made in the retinal margin to allow the retina to flatten. The retina was rinsed in 1× PBS and immunolabeled while free-floating. To observe the photoreceptor morphology in the *hrhoG/hrhoG* mice, the eyes were fixed in 4% formaldehyde in 1× PBS for 30 minutes, transferred to a slide, coverslipped with an antifade reagent (Prolong Gold; Molecular Probes, Eugene, OR), and examined by confocal microscope.

Antibodies and Antisera

The details of all primary antibodies are presented in Table 1. Secondary antisera were raised in donkey, were specific for either rabbit or goat immunoglobulins, and were conjugated to the fluorescent dyes AlexaFluor 488 and AlexaFluor 555 (dilution: 1:200–1:500; Molecular Probes).

Immunohistochemistry

Immunohistochemistry on retinal wholemounts were performed as described previously.[15,18] Wholemounts were treated with 1% to 2% $NaBH_4$ for 1 to 2 minutes, rinsed in deionized water followed by 1× PBS, and incubated in blocking solution for 1 hour at room temperature to block nonspecific labeling. The retinas were incubated in primary antibody for 3 days at 4°C. They were then were rinsed in 1×-PBS for 2 hours at room temperature and incubated free-floating in secondary antibody at room temperature for 1 hour. The retinas were rinsed in 1× PBS for 2 hours at room temperature, flattened onto microscope slides with the ganglion cell side up, coverslipped with antifade medium, and examined by confocal microscope.

Imaging

Confocal images were acquired with a confocal laser scanning microscope (LSM) with a krypton-argon laser (LSM 510; Carl Zeiss Meditec, Thornwood, NY). The images were captured with either 40× (numerical aperture, 1.30) or 63× (numerical aperture, 1.40) oil-immersion objective lenses. Stacks of serial optical sections were collected at a step size of 0.3 μm. Each image shown is either a maximum projection of an image stack, or a single, representative optical section processed with software (LSM; Carl Zeiss Meditec) and prepared with image-analysis software (Photoshop, ver. 6.0; Adobe Systems, San Jose, CA).

Image Analysis

Pupillary area was measured with ImageJ (ver. 1.37; developed by Wayne Rasband, National Institutes of Health, Bethesda, MD; available at http://rsb.info.nih.gov/ij/index.htm) by calculating the pupillary area (in square pixels) from each photograph with the elliptical selec-

Table 1. Antibodies and Antisera

	Host	Cat No.	Dilution	Source	Reference
Calretinin	Rabbit	CR 7699/4	1:5000	Swant, Bellinzona, Switzerland	16, 17
VChat	Goat	G448A	1:100	Promega, Madison, WI	—

tion tool (Fig. 1B). This measure was normalized to the similarly measured area enclosed by the limbus. The diameter of the limbus was measured after the termination of each experiment.

Results

Effects of Anesthesia and Mydriatics on the Time Course of Pupillary Dilation

The mydriasis after a loading dose of K+X anesthesia was rapid for the first 10 minutes (Figs. 1C, 1D, 1G; blue plot). The growth of pupillary diameter was insignificant beyond 20 minutes of induction of K+X anesthesia (Fig. 1E). The average pupillary diameter ($n = 4$) showed a small dip that started at ~48 to 50 minutes and troughed at ~70 minutes, correlating with the first maintenance dose of anesthesia administered at 40 to 45 minutes after induction. Atropine (A) was instilled into the cylindrical bath after 20 minutes of K+X injection, at which time the mydriasis caused by K+X alone had nearly reached its maximum. There was no significant difference in the mydriasis produced by K+X+A (Fig. 1G, green) compared

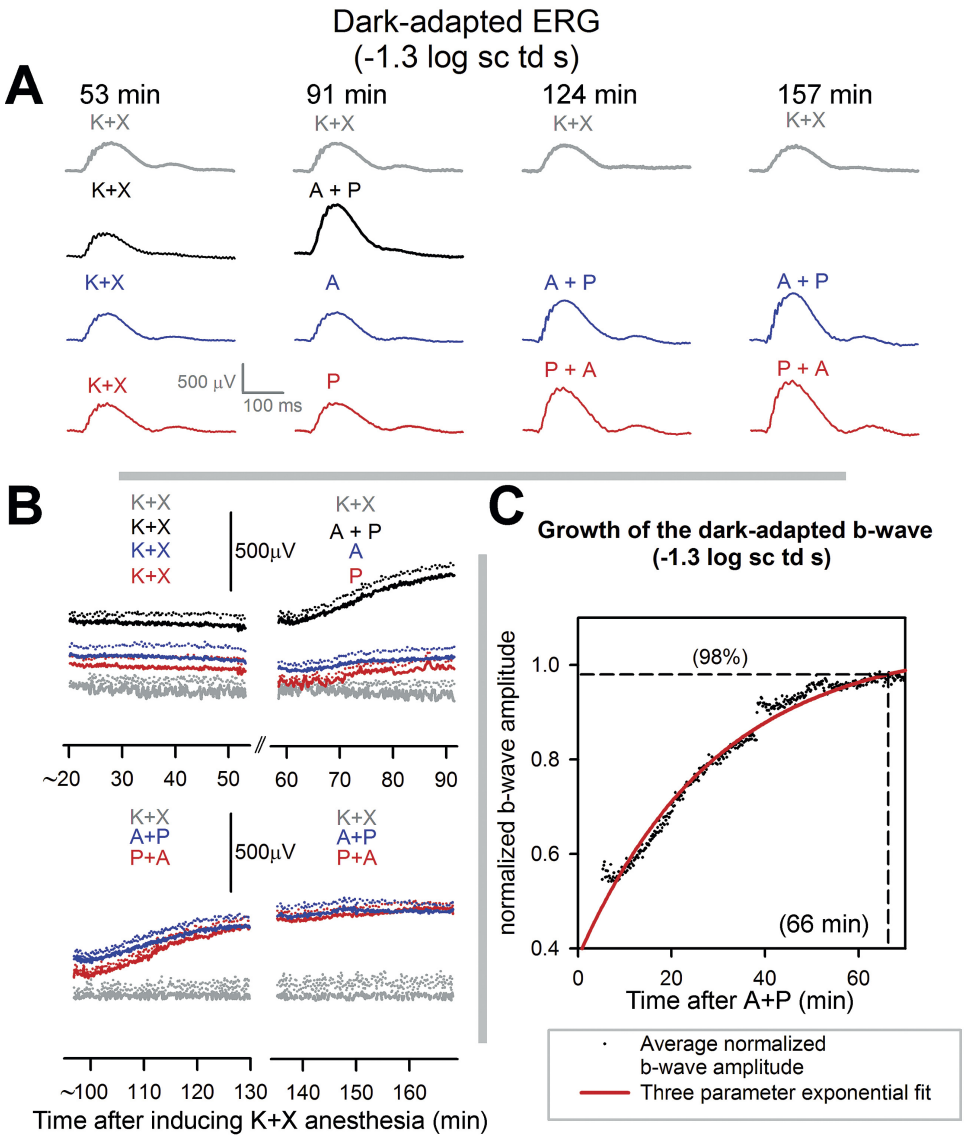

Figure 2. Time course of effects of mydriatics on the dark-adapted ERG of anesthetized mice: (**A**, *gray traces*) dark-adapted ERG of a single mouse recorded at 53, 91, 124, and 157 minutes after induction of anesthesia in response to flashes of −1.3 log sc td s. *Black traces*: dark-adapted ERG in response to flashes of −1.3 log sc td s for a single mouse at distinct time intervals. K+X: 53 minutes after induction of anesthesia; A+P: 91 minutes after induction of anesthesia and 38 minutes after instillation of topical A+P. *Blue traces*: dark-adapted ERG in response to flashes of −1.3 log sc td s for a single mouse at distinct time intervals. K+X: 53 minutes after induction of anesthesia; A: 91 minutes after induction of anesthesia and 38 minutes after instillation of topical A; A+P (*left*): 124 minutes after induction of anesthesia, 76 minutes after instillation of topical A, and 38 minutes after instillation of topical A+P. A+P (*right*): 157 minutes after induction of anesthesia, 109 minutes after instillation of topical A, and 71 minutes after instillation of topical A+P. *Red traces*: dark-adapted ERG in response to flashes of −1.3 log sc td s for a single mouse at distinct time intervals. K+X: 53 minutes after induction of anesthesia; P: 91 minutes after induction of anesthesia and 38 minutes after instillation of topical P; P+A (*left*): 124 minutes after induction of anesthesia, 76 minutes after instillation of topical P, and 38 minutes after instillation of topical A+P. P+A (*right*): 157 minutes after induction of anesthesia, 109 minutes after instillation of topical P, and 71 minutes after instillation of topical A+P. (**B**) Time course of change in dark-adapted b-wave amplitude (−1.3 log sc td s) after induction of K+X anesthesia. Each colored trace represents the same set of animals under observation after receiving K+X anesthesia, with or without mydriatics. The different data sets are offset vertically from one another, as the initial baselines for all them are indistinguishable. *Gray traces*, *top* and *bottom*: average b-wave amplitude of the dark-adapted ERG of three animals after K+X anesthesia. *Black traces* ($n = 3$), *top*: K+X: average b-wave amplitude since K+X anesthesia; A+P: average b-wave amplitude after administration of topical A+P after 54 minutes of K+X anesthesia. *Blue traces* ($n = 3$), *top*: K+X: average b-wave amplitude since K+X anesthesia; A: average b-wave amplitude after administration of topical A after 54 minutes of K+X anesthesia; *bottom*: A+P (*left*), average b-wave amplitude after topical A+P administered after 92 minutes of K+X anesthesia (39 minutes after A); A+P (*right*), traces continued from A+P (*left*). *Red traces* ($n = 4$), *top*: K+X, average b-wave amplitude since K+X anesthesia; P, average b-wave amplitude after administration of topical P after 54 minutes of K+X anesthesia; *bottom*: P+A (*left*), average b-wave amplitude after topical A+P administered after 92 minutes of K+X anesthesia (after 39 minutes after A); P+A (*right*), traces continued from A+P (*left*). *Dotted lines*: +1 SEM. (**C**) Time course of growth of the b-wave amplitude after coapplication of A+P. *Dots*: averaged b-wave amplitude ($n = 7$) normalized to the b-wave V_{max} (data from Fig. 2B, *red* and *blue traces*, *bottom*). *Dots* were fitted with an exponential with a time constant of 29.7 minutes (*gray curve*). *Horizontal dashed line*: 98% saturation of the fitted function, which corresponded to a time of 66 minutes after application of A+P (*vertical dashed line*).

with K+X alone. The small decrease in pupillary dilation induced by K+X anesthesia at 48 to 50 minutes was not observed in A-instilled eyes. Instillation of A at 20 minutes after K+X anesthesia and then a combination of A+P at 40 minutes after anesthesia produced similar amplitudes of mydriasis as did A instillation alone in the K+X-anesthetized mice (Fig. 1G, red plot). The pupillary dilation produced at the end of all three experimental paradigms was similar (Figs. 1E–G). We conclude that K+X anesthesia and mydriatics (used either singly or in combination) produce similar extents of mydriasis.

Effect of a Combination of A+P on the b-Wave Amplitude in K+X-Anesthetized Mice

Figure 2A shows representative waveforms (gray traces) from an animal recorded after K+X anesthesia at 53, 91, 124 and 157 minutes after induction. The waveforms recorded at 53, 91, and 124 minutes after anesthesia were very similar. The b-wave recorded at 132 minutes showed a decrease in amplitude. The average b-wave amplitude decreased by 11% beyond 130 minutes after K+X anesthesia, compared with the first 33 minutes of recording (Fig. 2B).

The black traces in Figure 2A show that representative ERG traces recorded at 38 minutes after application of topical A+P (91 minutes after induction) in a K+X-anesthetized mice were of significantly higher amplitudes compared with those recorded after 53 minutes after induction. At similar times after single application of either A (Fig. 2A, blue traces, top) or P (Fig. 2A, red traces) (i.e., 38 minutes after mydriatic and 91 minutes after induction), the ERG amplitudes were similar to those produced by K+X anesthesia alone. Application of either topical P after application of A (Fig. 2A, blue trace) or vice versa (Fig. 2A, red trace) produced significantly augmented ERGs as shown in the representative ERG waveforms recorded after 38 and 71 minutes after application of the mydriatic combination (i.e., 124 and 157 minutes after induction of K+X anesthesia).

The time course of the averaged b-wave amplitudes measured from the baseline to the b-wave peak for the various experimental protocols used in Figure 2A is illustrated in Figure 2B. The experiments commenced 20 minutes after induction of K+X anesthesia. The initial 33.3 minutes of recording shows the variation in b-waves observed after K+X anesthesia. Single application of either A or P resulted in similar b-wave amplitudes with no observable growth in b-wave amplitudes compared with their premydriatic-instilled control for a 33.3-minute recording session. However, application of both A+P produced a gradual but significant increase in the b-wave amplitudes compared with the premydriatic-instilled control ERGs for the same 33.3-minute recording session or ERGs recorded after application of a single mydriatic. To fully characterize this b-wave growth and to check whether it depended on the order of application of mydriatics we topically instilled a second mydriatic in those eyes that had received a single mydriatic, and ERGs were then recorded for the next 66.6 minutes (Fig. 2B, bottom panel). The ERG growth occurred only after a second mydriatic was instilled and was independent of the order of application. We did not observe any significant differences in time to peak or changes in the time course of the leading edge of the rod-driven b-wave response (see Supplementary Fig. S1, http://www.iovs.org/cgi/content/full/51/1/567/DC1).

Figure 2C plots the time course of change of the averaged normalized b-wave amplitude for the experimental paradigms which involved topical instillation of two mydriatics recorded over a 66-minute period (i.e., the blue and red traces in Fig. 2B, bottom). The data points were fitted by a three-parameter exponential approach to saturation (red curve):

$$\text{b-wave amplitude} = b_0 + (V_{max} - b_0)(1 - e^{\left(-\frac{1}{\tau}\cdot \text{time}\right)})$$

where, b_0 is normalized b-wave amplitude before drug effects, V_{max} is normalized maximum amplitude of the b-wave after A+P application, and τ is the time constant for the growth in b-wave amplitude. The parameters for the fit ($R^2 = 0.94$) were: $b_0 = 0.49$, $V_{max} = 1.06$, and $\tau = 29.7$ minutes corresponding to the growth in b-wave amplitude reaching 98% of its maximum value in 66 minutes after the application of a combination of A+P (this includes the 5 minutes of waiting time after application of the second mydriatic). Thus, we conclude that significant ERG amplitude growth occurs only after a combination of A+P is used and is independent of their order of application. Full growth is reached at 1 hour after application.

Roles of Duration of Anesthesia and Light Exposure in Growth of ERG

In another set of experiments, A+P was instilled in both eyes before anesthesia, and the animal was immediately anesthetized and kept in the dark for 1 hour (Fig. 3, top). The first flash produced a fully grown b-wave that remained at the same value for another half hour of recording. This result indicates that subjecting the eye to successive flashes was not a factor in the growth of the ERG. Rather, only the simultaneous presence of A+P in a K+X-anesthetized mice for a period was necessary. In another experiment A+P was topically applied to both eyes in a mouse 1 hour before anesthesia. In this case, ERGs recorded 20 minutes after induction of anesthesia produced a b-wave of ~500-μV amplitude that grew over a period of 1 hour (Fig. 3, bottom). Thus K+X anesthesia is required together with A+P over a period to produce an augmentation of the ERG. This experiment also excludes slow diffusion of topically applied mydriatics through the ocular media to the retina as the primary reason for the long time required for maximum growth of the b-wave.

Effects of Anesthesia and Mydriatics on the Voltage-Energy Relationship of the ERG

To characterize the effects of anesthesia and mydriatics on the voltage-energy relationship of the ERG it was important to remove the confound of a changing waveform and so the ERG was closely monitored for stability with repetitive test flashes of −1.3 log sc td s every 10 seconds after every mydriatic instillation. Once the ERG waveforms were stable, ERG responses to flashes of incrementally increased energies (−6.1 to 1.9 log sc td s) were recorded. Using this paradigm, we re-

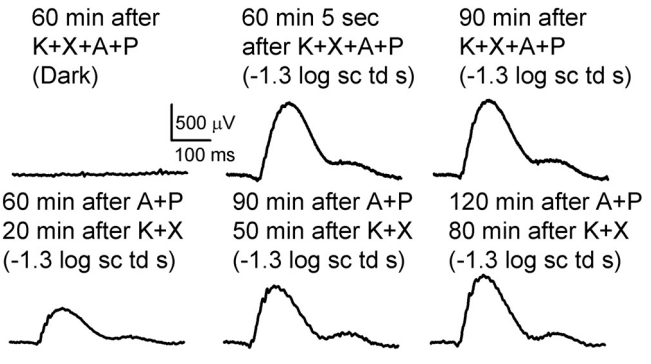

Figure 3. Duration of anesthesia was an important factor in producing growth of ERG. *Top* (*left*): ERG trace in the dark; (*middle* and *right*) ERG traces in response to −1.3-log sc td s flash. *Bottom*: ERG traces in response to −1.3-log sc td s flash.

corded consecutively the ERG responses after anesthesia, topical instillation of A and topical instillation of a combination of A+P. ERGs from a single representative animal are shown in Fig. 4A. The ERG responses for all flash energies after K+X anesthesia (Fig. 4, black traces) were very similar to those after topical A instillation in the anesthetized animal (blue traces). Combined instillation of A+P produced an increase in ERG amplitudes (Fig. 4, red trace). Dark-adapted ERG waveforms originating from the proximal inner-retina in response to very low flash energies, the negative- and positive-scotopic threshold response (nSTR and pSTR) were augmented in amplitude. These ERG waveforms are known to originate from inner retinal mechanisms in the amacrine and retinal ganglion cells.[19–22] The b-waves, known to originate primarily from the depolarization of rod bipolar cell for low flash energies (for example, −2.5 log sc td s) and both rod- and ON cone-bipolar cells for higher flash energies (for example, 1.6 log sc td s)[23] were also significantly increased in amplitude. The amplitude of the a-wave response (originating primarily from light evoked activity of rod photoreceptors in the murine retina) was also considerably increased (1.6 log sc td s; see Fig. 4A, inset). The averaged normalized ERG waveforms for this set of experiments are shown in Supplementary Figure S1. Although there was an augmentation of the total ERG waveform after a combination of A+P, the time-course of the ERG waveforms for the low and higher scotopic intensities were almost invariant (−4.0, −3.1, and −1.3 log sc td s). However, for higher intensities that involved active rod and cone circuits (1.6 log sc td s), resulted in a change in shape of the later part of the b-wave past its leading edge.

Figure 4B plots the b-wave amplitude measured at 110 ms as a function of scotopic-intensities for the dark-adapted ERG. The Fulton-Rushton hyperbolic equation[24] was used to fit the data to represent the scotopic PII, similar to another study[22]:

$$V = \frac{V_{max} \cdot I}{(I + I_0)}$$

where V is ERG response amplitude, V_{max} is the maximum amplitude of the response, I_0 is flash energy that elicits a

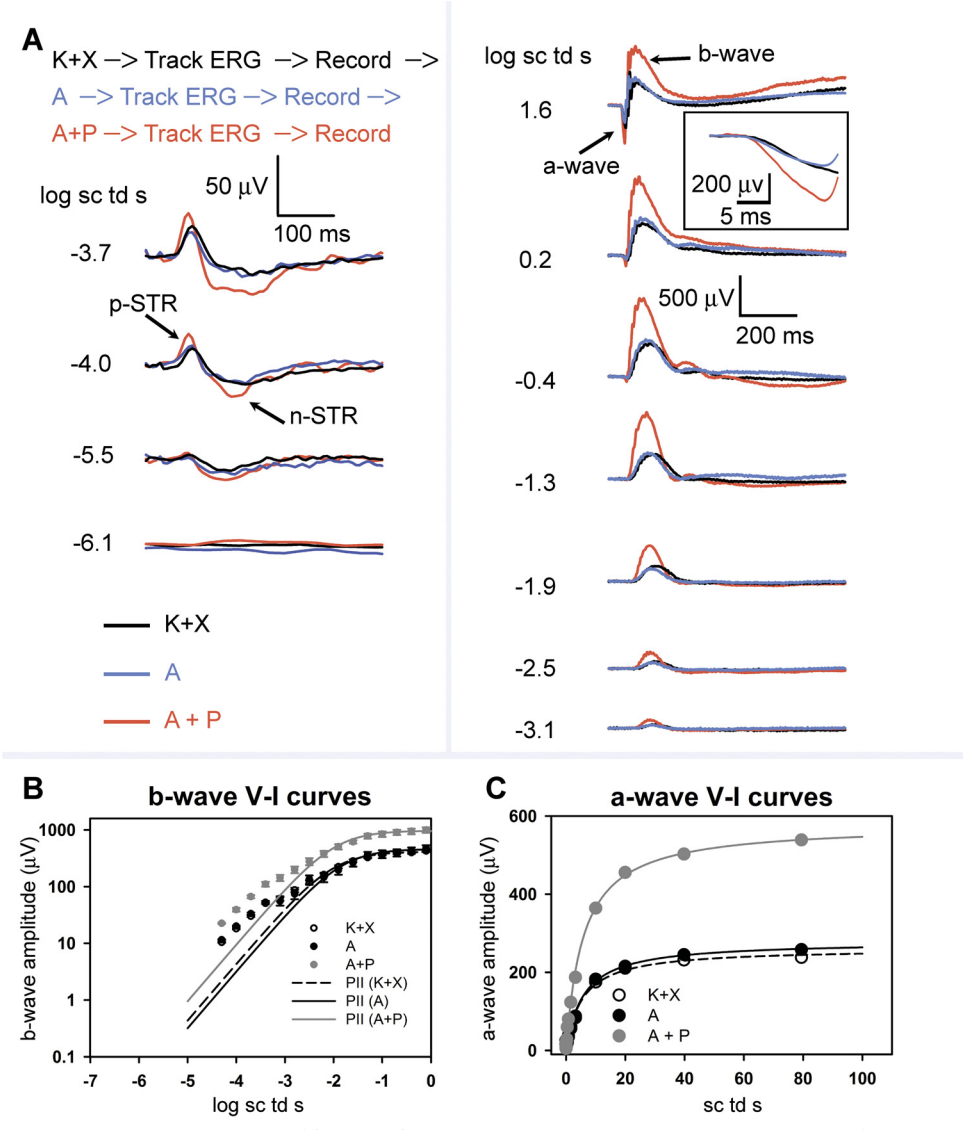

Figure 4. Dark-adapted ERG responses to brief full-field flashes of increasing energy after anesthesia and after consecutive topical application of A and A+P in anesthetized mice: (**A**) *Top*: order of events in this experimental paradigm. Track ERG: dark-adapted ERGs were tracked with −1.3-log sc td s flashes (0.2 Hz) until the responses were of uniform amplitude. Record: ERG responses to brief full-field flashes of increasing energy were recorded. Dark-adapted ERGs recorded in a single experimental session from a mouse after anesthesia (K+X) and after subsequent instillation of topical A followed by a combination of topical A+P. *Left*: ERG responses to low-energy flashes (from *bottom* to *top*: −6.1 to −3.7 log sc td s) shows augmentation of the negative scotopic threshold response (nSTR) and the positive STR (pSTR) (*arrows*) subsequent to topical application of A+P, but not to topical A in K+X-anesthetized mice. *Right*: ERG response to flashes of intermediate to high-energy (from *bottom* to *top*: −3.1 to 1.6 log sc td s) shows augmentation of the photoreceptor-derived a-wave and the ON bipolar cell–derived b-wave only subsequent to topical application of A+P but not for topical A in the K+X-anesthetized mice. *Inset*: the a-wave plotted on an expanded time-scale (1.6 log sc td s). (**B**) ERG b-wave amplitudes (group mean ± one SEM) plotted as a function of stimulus energy after K+X anesthesia and after subsequent instillation of topical A followed by a combination of topical A+P. The data-points, fitted with the Fulton-Rushton function represent the voltage-energy relationship of the PII after K+X anesthesia and PII after subsequent instillation of topical A, followed by a combination of topical A+P. (**C**) ERG a-wave amplitudes (group mean ± 1 SEM) plotted as a function of stimulus energy after K+X anesthesia and after subsequent instillation of topical A followed by a combination of topical A+P. The data-points were fitted with the Fulton-Rushton function to characterize the voltage-energy relationship for K+X anesthesia and after subsequent instillation of topical A followed by a combination of topical A+P.

half-maximum response, and I is flash energy that elicits the response, V.

Responses to flash energies between −4.5 to 0 log sc td s were used to produce the fit, to reduce the effects of the STRs in the fit for low intensities, and to minimize the influence of the cone-driven responses at higher intensities.[23] Even though the Fulton-Rushton equation does not provide a good fit for the curves at lower intensities, pharmacologic experiments involving blockade of inner-retinal circuitry with GABA has revealed that it can suitably represent the rod-bipolar cell–derived PII component of the b-wave originating from the light-evoked activity of rod-bipolar cells.[22] The sensitivity and V_{max} of the curve for the anesthetized animal (Fig. 4B, filled circles) and the anesthetized animal administered A (Fig. 4B, open circles) were almost indistinguishable. There was a greater than two-fold increase in the V_{max} (see Table 2) after topical application of a combination of A+P compared with A alone. However, the sensitivities for all three conditions were very similar. The unchanged sensitivity of the b-wave voltage-energy plots further verifies that mydriasis was not a factor in producing an increase in V_{max} after A+P application, consistent with our direct observations of the lack of effect of A+P on mydriasis. Our observations on the amplitudes and sensitivity of the b-wave are restricted only to the initial rising limb (rod-driven) of the b-wave, until its first saturation.

The a-wave amplitudes plotted as a function of stimulus energy are shown in Figure 4C. There was no significant difference in the V_{max} and sensitivity of the Fulton-Rushton fits for the a-wave energy-response function after K+X anesthesia and topical application of A after anesthesia. Combined application of A+P produced a greater than two-fold increase in the amplitude of the a-wave compared with topical application of A alone. Similar to the flash-energy response function for the b-wave, the sensitivity of the a-waves remained unaltered (Table 2).

Effect of a Combination of Mydriatics on Light-Evoked Inner Retinal Signaling in Severe Photoreceptor Degeneration

To characterize the effects of the combination of A+P on light-evoked signaling in states of retinal degeneration, we compared the ERG signals after topical application of A with those after topical application of P in K+X-anesthetized albino *hrhoG/hrhoG* mice. Previous studies have shown that mice whose native rhodopsin gene has been replaced with the corresponding human DNA modified to encode an enhanced GFP fusion at the C terminus of rhodopsin (*hrhoG/hrhoG* mice[11]) undergo severe progressive photoreceptor degeneration, such that there are virtually no photoreceptor outer segments by 3 to 5 months. We chose a time point of 7.5 months to record ERGs from four *hrhoG/hrhoG* mice, to ensure that the ERG records were taken when photoreceptor degeneration was very severe. Because these animals were albino, pupillary pigmentation was not expected to cause a significant alteration to the ERG.

Table 2. Parameters of the Fulton-Rushton Function for Dark-Adapted b- and a-Waves

Parameters	K+X	A	A+P
b-Wave (n = 4)			
V_{max} (μV)	413.58	460.66	969.79
I_0 (log sc td s)	−2.02	−1.87	−1.99
R^2	0.92	0.91	0.92
a-Wave (n = 4)			
V_{max} (μV)	261.20	278.99	578.59
I_0 (log sc td s)	0.73	0.76	0.76
R^2	0.99	0.99	0.99

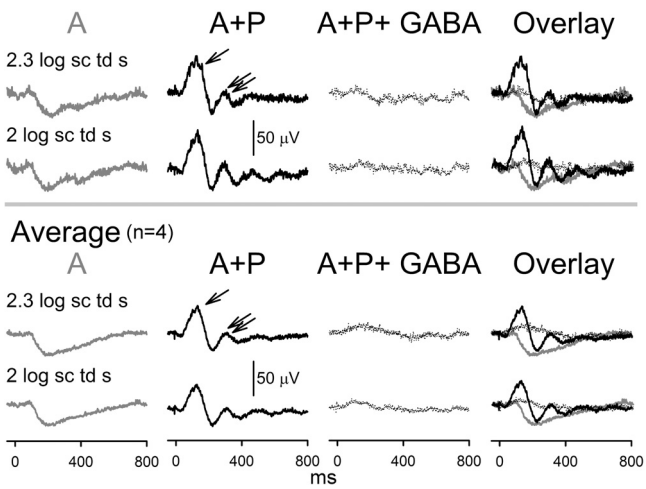

Figure 5. Dark-adapted ERG responses to full-field flashes after consecutive topical application of A and A+P and intravitreal GABA injection in 7.5-month-old *hRhoG/hRhoG* anesthetized mice: *Top*: dark-adapted ERGs in response to response saturating high-energy flashes (2–2.3 log sc td s) recorded in a single experimental session from a single anesthetized *hrhoG/hrhoG* mouse in the following temporal sequence from left to right: 30 minutes of instillation of topical A, 1 hour of instillation of topical A+P, and 1 hour of intravitreal injection of GABA in the A+P-instilled eye. *Bottom*: averaged dark-adapted ERGs in response to high-energy flashes (2–2.3 log sc td s) recorded from single experimental sessions from anesthetized *hrhoG/hrhoG* mice (n = 4) in the following temporal sequence from *left* to *right*: instillation of topical A, instillation of topical A+P, and intravitreal injection of GABA.

ERGs recorded from these animals (Fig. 5) produced low-amplitude (40 μV), slow (time to peak: 200 ms) electronegative signals for very high stimulus energies, with maximum amplitudes reached at 2 to 2.3 log sc td s. Similar dark-adapted electronegative ERG signals have been observed in other photoreceptor degeneration models such as RCS rat and are known to originate from light-evoked activity in the inner retina.[25] At 1 hour after instillation of a combination of A+P on the cornea, these electronegative waveforms were replaced by a waveform with two prominent positive peaks. The first positive peak was of larger amplitude (~50 μV, measured from base-line to peak) than the second one (~30 μV, measured from trough to peak). The first peak also had a faster time course (time to peak: 110–120 ms) than did the second peak (time to peak: 0.3 seconds). There were minor peaks visible at later times in the record. Intravitreal GABA injection extinguished these waveforms to be replaced by a very low-amplitude (~10 μV), positive potential (time to peak, 110–120 ms), indicating that the oscillating waveform produced by A+P treatment arose from electrical activity in the inner retina. This low-amplitude positive potential most likely represents the residual PII. We conclude that a combination of A+P results in alteration of inner retinal potentials (probably originating proximal to retinal bipolar cells) in a photoreceptor-degenerated retina. Confocal microscopy showed the presence of a sparse population of photoreceptors that lacked visible outer segments (Supplementary Fig. S2A–D, http://www.iovs.org/cgi/content/full/51/1/567/DC1). Calretinin and VChat immunofluorescence was present in the neurons in the proximal inner nuclear and ganglion cell layers, indicating the presence of viable inner retinal neurons and cholinergic cells (Supplementary Fig. S2E–G).

Discussion

We found that a combination of K+X can produce mydriasis in mice in the anesthetic doses used in this study, very likely by stimulation of the α_2-adrenergic receptors in the iris and central nervous system (CNS) in a dose-dependent manner, as seen in rats.[26] Although K+X anesthesia can produce mydriasis, variations in the extent of mydriasis can occur, possibly due to the changing systemic anesthetic concentration. At least one mydriatic is necessary to maintain the constancy of pupillary dilation while recording ERGs over a prolonged duration (i.e., >40–45 minutes from the initial loading dose in our case).

Anticholinergic drugs and adrenergic agonists have been reported to influence the electroretinogram individually in rabbits,[27,28] but we found no evidence of significant alteration of the ERG b-wave with the singular use of A in K+X-anesthetized mice compared with K+X anesthesia alone. The major waves of the ERG, the photoreceptor-derived a-wave and the ON bipolar cell–derived b-wave, had increased amplitudes but no change in sensitivity after stable ERG recording after a combination of A+P in K+X-anesthetized mice. Although the exact mechanism for producing these effects remains to be determined, the most economical explanation for these changes in the ERG is that the combined effects of muscarinic antagonism and α-adrenergic agonism in mice that were anesthetized with K+X, resulted in a decrease in resistance across the retina at least for the rod-driven ERGs where the waveforms were invariant in their time course. This decrease in resistance could potentially occur by altering the conductances of ion channels involved in light-evoked signaling in retinal neurons. Changes in the resistance of other ocular structures can affect the ERG amplitudes (e.g., retinal pigment epithelium[29–32]; vitreous[33,34]). However, the effects of the drugs on the light-evoked waveforms, for dark-adapted ERGs involving both rod and cone circuits, and in the mice exhibiting advanced retinal degeneration cannot be explained simply by a decrease in resistance, suggesting that changes in responses in individual retinal cell types are involved.

The ERG augmentation requires the presence of a combination of A+P in K+X-anesthetized mice for an extended period. The slow growth of the waveforms could not be a result of slow diffusion of A+P, because A+P application 1 hour before K+X anesthesia did not produce a fully grown b-wave when ERGs were recorded 20 minutes after K+X anesthesia. Moreover, extended duration of K+X anesthesia is not by itself responsible for the slow augmentation of the ERG, because even when the animal was anesthetized with K+X for an hour, slow growth of the ERGs occurred only after topical application of A+P. These results suggest that the interaction of mydriatic combination with anesthesia probably triggered a secondary slowly evolving mechanism that was responsible for producing the augmentation of the ERG waveforms. Because topical mydriatics are known to enter the systemic circulation and cause side effects,[3,4] the route by which a combination of mydriatics could produce its effect on the retina could be either via the systemic circulation or via diffusion across the cornea, anterior chamber, and vitreous (for example, Refs. 35, 36). The slowly evolving nature of the drug-induced changes is suggestive of effects on paracrine or endocrine mechanisms within the retina or elsewhere in the body. Paracrine mechanisms in the retina that produce an augmentation of the ERG waveforms have been reported in amacrine cells that release dopamine, a global modulator of retinal activity that is known to produce a change in all the major ERG waves (for review, see Ref. 37). Patients with Parkinson's disease, who are reported to have low retinal dopamine levels,[38] manifest abnormally high-amplitude ERG waveforms when untreated, but the amplitudes rapidly revert to normal levels with L-DOPA treatment.[39] Although it is not obvious how muscarinic antagonists and α-adrenergic agonists in the presence of K+X anesthesia could affect the dopaminergic amacrine cells in the murine retina, the receptor types on which they act are known to be closely related to dopaminergic amacrine cell activity in different species (for example, guinea-pig[40]; tiger salamander and chicks[41,42]; and rats[43]). Ketamine is an antagonist for NMDA receptors that are known to be distributed mainly in the inner retinal neurons (for review, see Ref. 44). Although blockade of NMDA receptors itself is not known to cause a significant change in the rodent ERG,[19] it may do so indirectly in combination with other mechanisms. Xylazine, an α2-adrenergic receptor agonist, may add somewhat to the effects produced by phenylephrine, a nonspecific α-adrenergic receptor agonist. Cholinergic amacrine cells ([45–49]) and epinephrine-containing amacrine cells ([50–52]) are endogenous sources of acetylcholine and epinephrine in the retina. Expression of both α-adrenergic and cholinergic receptors has been reported in retina of various species (for example, α-adrenergic receptors[53–61] and muscarinic receptors[62,63]). It seems likely that both acetylcholine and adrenergic systems have modulatory functions in the retina and could affect neuronal systems that could influence the generators of the a- and b-waves, either directly or indirectly, which may have been unmasked with the use of K+X anesthesia. The possibility of systemic effects on the ERG after these pharmacologic combinations cannot be ruled out, given the fact that substances such as corticosteroids or high levels of carbon dioxide can lead to an augmented ERG response.[64,65]

We found that the ERG response characteristics for the topically administered A+P combination in K+X-anesthetized mice with severe photoreceptor degeneration was remarkably different from those observed after topical administration of A alone. Recording ERGs in albino mice ensured that the changes observed were not a consequence of variable pupillary dilation in this animal. The conversion of an electronegative potential in response to saturating light to a waveform with positive potentials on administration of the A+P combination cannot be explained on the basis of a decreased light-evoked resistance. The altered waveform seen after a combination of mydriatics originated in the inner retina indicating that in states of photoreceptor degeneration mydriatic combination could potentially alter inner retinal signaling. The presence of a very small PII remnant after GABA injection conforms to a previous finding that there was a relative lack of functioning bipolar cells in this degenerated retina.[66] The combination of A+P most likely caused an alteration of light-evoked signaling in the extremely active amacrine and ganglion cell circuits.[66] Another significant implication of our finding is that a standardized mydriatic protocol is needed for ERG recording in pathologic conditions, perhaps with the inclusion of only one mydriatic agent.

Considerable additional work will be needed to determine the mechanism(s) and site(s) of action of the effects we have observed and to determine the extent to which they occur in other species, including humans. The extensive use of related drugs, including anticholinergic drugs, adrenergic agonists, and NMDA antagonists for a range of therapeutic and diagnostic applications, and their dramatic effects on the ERG argue that these efforts are well warranted.

References

1. Moroi SE, Lichter PR. Ocular Pharmacology. In: Goodman LS, Hardman JG, Limbird LE, Gilman AG, eds. *Goodman & Gilman's the Pharmacological Basis of Therapeutics.* New York: McGraw-Hill; 2001:xxvii, 2148.

2. Bartlett JD, Jaanus SD. *Clinical Ocular Pharmacology*. 5th ed. Oxford, UK: Butterworth-Heinemann; 2008:xvi, 793.
3. Isenberg S, Everett S. Cardiovascular effects of mydriatics in low-birth-weight infants. *J Pediatr.* 1984;105:111–112.
4. Mirmanesh SJ, Abbasi S, Bhutani VK. Alpha-adrenergic bronchoprovocation in neonates with bronchopulmonary dysplasia. *J Pediatr.* 1992;121:622–625.
5. Harrison NL, Simmonds MA. Quantitative studies on some antagonists of N-methyl D-aspartate in slices of rat cerebral cortex. *Br J Pharmacol.* 1985;84:381–391.
6. Schwartz DD, Clark TP. Affinity of detomidine, medetomidine and xylazine for alpha-2 adrenergic receptor subtypes. *J Vet Pharmacol Ther.* 1998;21:107–111.
7. Peachey NS, Ball SL. Electrophysiological analysis of visual function in mutant mice. *Doc Ophthalmol.* 2003;107:13–36.
8. Weymouth AE, Vingrys AJ. Rodent electroretinography: methods for extraction and interpretation of rod and cone responses. *Prog Retin Eye Res.* 2008;27:1–44.
9. Lyubarsky AL, Daniele LL, Pugh EN Jr. From candelas to photoisomerizations in the mouse eye by rhodopsin bleaching in situ and the light-rearing dependence of the major components of the mouse ERG. *Vision Res.* 2004;44:3235–3251.
10. Mojumder DK, Qian Y, Wensel TG. Two R7 regulator of G-protein signaling proteins shape retinal bipolar cell signaling. *J Neurosci.* 2009;29:7753–7765.
11. Chan F, Bradley A, Wensel TG, Wilson JH. Knock-in human rhodopsin-GFP fusions as mouse models for human disease and targets for gene therapy. *Proc Natl Acad Sci U S A.* 2004;101:9109–9114.
12. Dawson WW, Trick GL, Litzkow CA. Improved electrode for electroretinography. *Invest Ophthalmol Vis Sci.* 1979;18:988–991.
13. Sagdullaev BT, DeMarco PJ, McCall MA. Improved contact lens electrode for corneal ERG recordings in mice. *Doc Ophthalmol.* 2004;108:181–184.
14. Mojumder DK. Capillary-contacting horizontal cells in the rodent retina. *J Anat Soc India.* 2008;57:34–36.
15. Mojumder DK, Wensel TG, Frishman LJ. Subcellular compartmentalization of two calcium binding proteins, calretinin and calbindin-28 kDa, in ganglion and amacrine cells of the rat retina. *Mol Vis.* 2008;14:1600–1613.
16. Pasteels B, Rogers J, Blachier F, Pochet R. Calbindin and calretinin localization in retina from different species. *Vis Neurosci.* 1990;5:1–16.
17. Winsky L, Nakata H, Martin BM, Jacobowitz DM. Isolation, partial amino acid sequence, and immunohistochemical localization of a brain-specific calcium-binding protein. *Proc Natl Acad Sci U S A.* 1989;86:10139–10143.
18. Mojumder DK, Frishman LJ, Otteson DC, Sherry DM. Voltage-gated sodium channel alpha-subunits Na (v) 1.1, Na (v) 1.2, and Na (v) 1.6 in the distal mammalian retina. *Mol Vis.* 2007;13:2163–2182.
19. Bui BV, Fortune B. Ganglion cell contributions to the rat full-field electroretinogram. *J Physiol.* 2004;555:153–173.
20. Mojumder DK, Sherry DM, Frishman LJ. Contribution of voltage-gated sodium channels to the b-wave of the mammalian flash electroretinogram. *J Physiol.* 2008;586:2551–2580.
21. Naarendorp F, Sieving PA. The scotopic threshold response of the cat ERG is suppressed selectively by GABA and glycine. *Vision Res.* 1991;31:1–15.
22. Saszik SM, Robson JG, Frishman LJ. The scotopic threshold response of the dark-adapted electroretinogram of the mouse. *J Physiol.* 2002;543:899–916.
23. Toda K, Bush RA, Humphries P, Sieving PA. The electroretinogram of the rhodopsin knockout mouse. *Vis Neurosci.* 1999;16:391–398.
24. Fulton AB, Rushton WA. Rod ERG of the mudpuppy: effect of dim red backgrounds. *Vision Res.* 1978;18:785–792.
25. Machida S, Raz-Prag D, Fariss RN, Sieving PA, Bush RA. Photopic ERG negative response from amacrine cell signaling in RCS rat retinal degeneration. *Invest Ophthalmol Vis Sci.* 2008;49:442–452.
26. Hsu WH, Lee P, Betts DM. Xylazine-induced mydriasis in rats and its antagonism by alpha-adrenergic blocking agents. *J Vet Pharmacol Ther.* 1981;4:97–101.
27. Nakagawa T, Kurasaki S, Masuda T, Ukai K, Kubo S, Kadono H. Effects of some psychotropic drugs on the b-wave of the electroretinogram in isolated rabbit retina. *Jpn J Pharmacol.* 1988;46:97–100.
28. Czepita D. Influence of alpha and beta-adrenergic stimulators and blockers on the electroretinogram and visually evoked potentials of the rabbit. *Biomed Biochim Acta.* 1990;49:509–513.
29. Brindley GS. The passive electrical properties of the frog's retina, choroid and sclera for radial fields and currents. *J Physiol.* 1956;134:339–352.
30. Brindley GS, Hamasaki DI. The properties and nature of the R membrane of the frog's eye. *J Physiol.* 1963;167:599–606.
31. Byzov AL. Localization of the R-membrane in the frog eye by means of an electrode marking method. *Vision Res.* 1968;8:697–700.
32. Ogden TE, Ito H. Avian retina. II. An evaluation of retinal electrical anisotropy. *J Neurophysiol.* 1971;34:367–373.
33. Arden GB, Brown KT. Some properties of components of the cat electroretinogram revealed by local recording under oil. *J Physiol.* 1965;176:429–461.
34. Doslak MJ, Plonsey R, Thomas CW. The effects of variations of the conducting media inhomogeneities on the electroretinogram. *IEEE Trans Biomed Eng.* 1980;27:88–94.
35. Kaiser T, Werner A, Baumer W, Kietzmann M. Tissue distribution of dexamethasone in canine ocular compartments following topical application of dexamethasone-21-isonicotinate and oxytetracycline HCl. *Vet Ophthalmol.* 2008;11:335–339.
36. Mizuno K, Koide T, Shimada S, Mori J, Sawanobori K, Araie M. Route of penetration of topically instilled nipradilol into the ipsilateral posterior retina. *Invest Ophthalmol Vis Sci.* 2009;50(6):2839–2847.
37. Witkovsky P. Dopamine and retinal function. *Doc Ophthalmol.* 2004;108:17–40.
38. Harnois C, Di Paolo T. Decreased dopamine in the retinas of patients with Parkinson's disease. *Invest Ophthalmol Vis Sci.* 1990;31:2473–2475.
39. Terziivanov D, Filipova M, Janku I, Balik J, Filip V, Stika L. Changes in electroretinogram and serum potassium during L-DOPA treatment in parkinsonism. *Arch Psychiatr Nervenkr.* 1983;232:507–513.
40. Weber B, Schlicker E. Modulation of dopamine release in the guinea-pig retina by G (i)- but not by G (s)- or G (q)-protein-coupled receptors. *Fundam Clin Pharmacol.* 2001;15:393–400.
41. Hare WA, Owen WG. Similar effects of carbachol and dopamine on neurons in the distal retina of the tiger salamander. *Vis Neurosci.* 1995;12:443–455.
42. Schwahn HN, Kaymak H, Schaeffel F. Effects of atropine on refractive development, dopamine release, and slow retinal potentials in the chick. *Vis Neurosci.* 2000;17:165–176.
43. Iuvone PM, Rauch AL. Alpha 2-adrenergic receptors influence tyrosine hydroxylase activity in retinal dopamine neurons. *Life Sci.* 1983;33:2455–2463.
44. Shen Y, Liu XL, Yang XL. N-methyl-D-aspartate receptors in the retina. *Mol Neurobiol.* 2006;34:163–179.
45. O'Malley DM, Sandell JH, Masland RH. Co-release of acetylcholine and GABA by the starburst amacrine cells. *J Neurosci.* 1992;12:1394–1408.
46. Voigt T. Cholinergic amacrine cells in the rat retina. *J Comp Neurol.* 1986;248:19–35.
47. Masland RH, Cassidy C. The resting release of acetylcholine by a retinal neuron. *Proc R Soc Lond B Biol Sci.* 1987;232:227–238.
48. Masland RH, Mills JW, Cassidy C. The functions of acetylcholine in the rabbit retina. *Proc R Soc Lond B Biol Sci.* 1984;223:121–139.
49. Hayden SA, Mills JW, Masland RM. Acetylcholine synthesis by displaced amacrine cells. *Science.* 1980;210:435–437.
50. Hadjiconstantinou M, Mariani AP, Panula P, Joh TH, Neff NH. Immunohistochemical evidence for epinephrine-containing retinal amacrine cells. *Neuroscience.* 1984;13:547–551.

51. Osborne NN. Noradrenaline, a transmitter candidate in the retina. *J Neurochem.* 1981;36:17–27.
52. Malmfors T. Evidence of adrenergic neurons with synaptic terminals in the retina of rats demonstrated with fluorescence and electron microscopy. *Acta Physiol Scand.* 1963;58:99–100.
53. Wikberg-Matsson A, Uhlen S, Wikberg JE. Characterization of alpha(1)-adrenoceptor subtypes in the eye. *Exp Eye Res.* 2000;70:51–60.
54. Matsuo T, Cynader MS. Localization of alpha-2 adrenergic receptors in the human eye. *Ophthalmic Res.* 1992;24:213–219.
55. Kalapesi FB, Coroneo MT, Hill MA. Human ganglion cells express the alpha-2 adrenergic receptor: relevance to neuroprotection. *Br J Ophthalmol.* 2005;89:758–763.
56. Ishimoto I, Kiyama H, Hamano K, et al. Co-localization of adrenergic receptors and vitamin-D-dependent calcium-binding protein (calbindin) in the dopaminergic amacrine cells of the rat retina. *Neurosci Res.* 1989;7:257–263.
57. Kiyama H, Tohyama M. Morphological demonstration of retinal neuroreceptors and mRNA: immunohistochemical demonstration of adrenergic receptor and visualization of preprotachykinin A mRNA by in situ hybridization histochemistry. *Neurosci Res Suppl.* 1988;8:S167–S181.
58. Lograno MD, Tricarico D, Masciopinto V, Scuderl AC. Specific binding of nicergoline on an alpha1-like adrenoreceptor in the rat retina. *J Pharm Pharmacol.* 2000;52:207–211.
59. Wikberg-Matsson A, Wikberg JE, Uhlen S. Characterization of alpha 2-adrenoceptor subtypes in the porcine eye: identification of alpha 2A-adrenoceptors in the choroid, ciliary body and iris, and alpha 2A- and alpha 2C-adrenoceptors in the retina. *Exp Eye Res.* 1996;63:57–66.
60. Berlie JR, Iversen LJ, Blaxall HS, Cooley ME, Chacko DM, Bylund DB. Alpha-2 adrenergic receptors in the bovine retina: presence of only the alpha-2D subtype. *Invest Ophthalmol Vis Sci.* 1995;36:1885–1892.
61. Woldemussie E, Wijono M, Pow D. Localization of alpha 2 receptors in ocular tissues. *Vis Neurosci.* 2007;24:745–756.
62. Wasselius J, Johansson K, Bruun A, Zucker C, Ehinger B. Correlations between cholinergic neurons and muscarinic m2 receptors in the rat retina. *Neuroreport.* 1998;9:1799–1802.
63. Yamada ES, Dmitrieva N, Keyser KT, Lindstrom JM, Hersh LB, Marshak DW. Synaptic connections of starburst amacrine cells and localization of acetylcholine receptors in primate retinas. *J Comp Neurol.* 2003;461:76–90.
64. Heckenlively JR, Nusinowitz S. Hyperabnormal (supranormal) electroretinographic responses. In: Heckenlively JR, Arden GB, eds. *Principles and Practice of Clinical Electrophysiology of Vision.* The MIT Press, Cambridge, MA; 2006:533–540.
65. Tanabe J, Shirao Y, Oda N, Kawasaki K. Evaluation of retinal integrity in eyes with retained intraocular metallic foreign body by ERG and EOG. *Doc Ophthalmol.* 1992;79:71–78.
66. Marc RE, Jones BW, Anderson JR, et al. Neural reprogramming in retinal degeneration. *Invest Ophthalmol Vis Sci.* 2007;48:3364–3371.